MOLECULAR AND CELLULAR BIOLOGY, Sept. 2008, p. 5381–5390 Vol. 28, No. 17
0270-7306/08/$08.00+0 doi:10.1128/MCB.00651-08

Sumo-1 Function Is Dispensable in Normal Mouse Development▽‡

Fu-Ping Zhang,[1]† Laura Mikkonen,[1]† Jorma Toppari,[2] Jorma J. Palvimo,[3] Irma Thesleff,[4] and Olli A. Jänne[1,5]*

Biomedicum Helsinki, Institute of Biomedicine (Physiology), University of Helsinki, FI-00014 Helsinki, Finland[1]; Departments of Physiology and Pediatrics, University of Turku, FI-20520 Turku, Finland[2]; Department of Medical Biochemistry, University of Kuopio, FI-70211 Kuopio, Finland[3]; Institute of Biotechnology, University of Helsinki, FI-00014 Helsinki, Finland[4]; and Department of Clinical Chemistry, Helsinki University Central Hospital, FI-00290 Helsinki, Finland[5]

Received 22 April 2008/Returned for modification 24 May 2008/Accepted 9 June 2008

To elucidate SUMO-1 functions in vivo, we targeted by homologous recombination the last three exons of the murine *Sumo-1* gene. *Sumo-1* mRNA abundance was reduced to one-half in heterozygotes and was undetectable in *Sumo-1*$^{-/-}$ mice, and SUMO-1-conjugated RanGAP1 was detectable in wild-type mouse embryo fibroblasts (MEFs) but not in *Sumo-1*$^{-/-}$ MEFs, indicating that gene targeting yielded *Sumo-1*-null mice. *Sumo-1* mRNA is expressed in all tissues of wild-type mice, and its abundance is highest in the testis, brain, lungs, and spleen. *Sumo-2* and *Sumo-3* mRNAs are also expressed in all tissues, but their abundance was not upregulated in *Sumo-1*-null mice. The development and function of testis are normal in the absence of *Sumo-1*, and *Sumo-1*$^{-/-}$ mice of both sexes are viable and fertile. In contrast to a previous report (F. S. Alkuraya et al., Science 313:1751, 2006), we did not observe embryonic or early postnatal demise of *Sumo-1*-targeted mice; genotypes of embryos and 21-day-old mice were of predicted Mendelian ratios, and there was no defect in lip and palate development in *Sumo-1*$^{+/-}$ or *Sumo-1*$^{-/-}$ embryos. The ability of *Sumo-1*$^{-/-}$ MEFs to differentiate into adipocyte was not different from that of wild-type MEFs. Collectively, our results support the notion that most, if not all, SUMO-1 functions are compensated for in vivo by SUMO-2 and SUMO-3.

Small ubiquitin-related modifier 1 (SUMO-1) is a member of the ubiquitin-related protein family (15, 16, 19, 23, 24). SUMO proteins are ubiquitously expressed throughout the eukaryotic kingdom. The yeast *Caenorhabditis elegans* and *Drosophila melanogaster* have a single *SUMO* gene, but other organisms, such as vertebrates and plants, have several *SUMO* genes. Four SUMO family members, SUMO-1 to SUMO-4, have been found in mammals. SUMO-4 precursor cannot be processed for substrate conjugation in vivo, and it may function exclusively through noncovalent interactions (27). SUMO-2 to SUMO-4 share greater amino acid sequence identity with each other than with SUMO-1. SUMO-1 to SUMO-3 have a wide tissue distribution, whereas SUMO-4 expression is limited to the kidneys, lymph nodes, and spleen (10, 21). SUMO-1, a 97-amino-acid-residue mature polypeptide, shares 18% sequence identity with ubiquitin, and the two proteins have similar three-dimensional structures. Like ubiquitin, SUMO is covalently conjugated to substrates by an isopeptide bond through the carboxyl terminus.

A consensus SUMO acceptor site, comprising the sequence ΨKXE (where "Ψ" is a large hydrophobic amino acid and K is the SUMO attachment residue) has been identified, although nonconsensus acceptor sites are also used for SUMO conjugation (15, 16). In addition, biological functions have been assigned to SUMO paralogues that are not covalently attached to substrate proteins (13). Many nuclear receptors, including androgen, progesterone, and glucocorticoid receptors, contain SUMO acceptor sites, suggesting a role for sumoylation in their signaling (18). Sumoylation is an evolutionarily conserved pathway from yeast to humans. SUMO is first activated by an E1 activating enzyme, the Aos1/Uba2 heterodimer, subsequently transferred to the unique E2 conjugating enzyme Ubc9, and conjugated to substrates in a reaction facilitated by different E3 ligases, including members of the PIAS family, RanBP2 nucleoporin, and polycomb protein Pc2. SUMO modification is a dynamic, reversible process, and distinct enzymes are responsible for SUMO conjugation and deconjugation. Several SUMO-specific proteases, including SENP1 (SuPr-2), SENP2 (SuPr-1), SENP3 (SMT3IP1), SENP5, and SENP6 (SUSP1), have been identified and localized (16, 17).

Sumoylation is an important control process in numerous biological events. SUMO modifications have been associated with many disease conditions, ranging from neurodegeneration to diabetes and inflammation (9, 16), as well as linked to the pathogenesis of several disorders, including Alzheimer's disease, Huntington's disease, and cancer (1, 9, 13, 21). Ubiquitin and ubiquitin-related proteins, such as SUMO paralogues, are important in diverse reproductive functions, including gametogenesis, ovulation, and steroid receptor activity (7, 8, 11, 36, 40). In *C. elegans*, the reproductive system is a major SUMO target during postembryonic development, and SUMO is required for gonadal and uterine-vulval morphogenesis (8). Knockdown of the single *SUMO* gene or the single *Ubc9* gene in *C. elegans* resulted in embryonic arrest after gastrulation and pleiotropic defects in larval development (20). Ubc9 function is mandatory for embryonic development in mammals, since *Ubc9*-null mouse embryos die at early postimplantation stage (26).

It was recently reported that *SUMO-1* haploinsufficiency

* Corresponding author. Mailing address: University of Helsinki, Institute of Biomedicine (Physiology), Biomedicum Helsinki, P.O. Box 63 (Haartmaninkatu 8), FI-00014 Helsinki, Finland. Phone: 358-9-19125040. Fax: 358-9-19125047. E-mail: olli.janne@helsinki.fi.

† F.-P.Z. and L.M. contributed equally to this study.

‡ Supplemental material for this article may be found at http://mcb.asm.org/.

▽ Published ahead of print on 23 June 2008.

causes cleft lip and/or palate (3). A patient with cleft lip and palate carried a translocation between human chromosomes 2q and 8q, and the breakpoint on chromosome 2 interrupted the *SUMO-1* sequence. A mouse line with gene trap targeting of *Sumo-1* exhibited cleft palate development with low penetrance in heterozygote mice, whereas homozygote embryos showed early lethality before closure of the palate (3).

To elucidate the in vivo roles of SUMO-1 in mammals, we knocked out *Sumo-1* in mice. Characterization of the mutant mice indicates that *Sumo-1* is dispensable in normal development and adult life and that most, if not all, SUMO-1 functions are compensated for by other SUMO paralogues. Importantly, we failed to detect any defect in palate development in *Sumo-1*$^{+/-}$ or *Sumo-1*$^{-/-}$ embryos.

MATERIALS AND METHODS

Genomic clone isolation. A genomic fragment of the *Sumo-1* gene spanning exons 3, 4, and 5, 2.2 kb of the flanking intron 2 and 1.8 kb of 3′-flanking region was isolated from 129/ola mouse cosmid library (RZPD, Heidelberg, Germany) by using a cDNA probe corresponding to exons 3, 4, and 5 of *Sumo-1*. DNA sequencing confirmed the identity of the genomic clone.

Targeting vector construction. The targeting plasmids pKO Scramber913, pKO SelectNeo V800, and pKO SelectTK V830 were purchased from Lexicon Genetics, Inc. (The Woodlands, TX). The *Sumo-1* targeting vector comprised the 2.2-kb intron 2 fragment as the 5′-homology region, the 1.8-kb 3′-flanking fragment as the 3′-homology region, a positive selection marker (the PGK-Neo expression cassette), and an MC1-tk (thymidine kinase) expression cassette (Fig. 1A).

ES cell culture. AB.2.2-prime embryonic stem (ES) cells (derived from mouse strain 129/SvEv) and primary mouse embryonic fibroblasts (MEFs) were from Lexicon Genetics, Inc. (Woodlands, TX) and Cell and Molecular Technologies, Inc. (Phillipsburg, NJ), respectively. ES cells were cultured on neomycin-resistant primary embryonic fibroblast feeder layers, and 10^6 cells were electroporated (500 μF, 240 V) with 30 μg of linearized targeting construct. After electroporation, the cells were plated on 100-mm culture dishes and exposed to G418 (300 μg/ml; Sigma) and ganciclovir (1 μM; Sigma) for 8 to 9 days. Colonies were picked and grown on 24-well dishes for 5 to 6 days, and about one-eighth of a colony was replated onto 24-well dishes for genomic DNA isolation, with the remainder being frozen at −80°C until further use.

Screening of targeted clones. DNA isolated from ES cell clones was screened by PCR, which produced a 2.2-kb fragment with a primer pair corresponding to the 5′ end of pGKneo (Neo1, 5′-CCACCAAAGAACGGAGCCGGTT-3′) and the 3′ end of *Sumo-1* (SUMO-1,P2, 5′-ACAGCCAGGGGTTACCTTGA-3′). Correct targeting was confirmed by Southern blot analysis of HindIII-digested DNA with probe 3 specific for the 3′-flanking region of *Sumo-1* (Fig. 1A); the expected fragment sizes were 8.2 kb for targeted *Sumo-1* and 3.6 kb for the authentic *Sumo-1*.

Mouse breeding. Morula aggregation was used to produce chimeric mice. Chimeras were identified by coat color, and males were subsequently bred to ICR females. Genotyping was performed by PCR with primer pairs for the wild-type allele (SUMO-1,P1, 5′-CTCAAACAACAGACCTGATTGC-3′; SUMO-1,P3, 5′-CACTATGGATAAGACCTGTGAATT-3′) and for the targeted allele (Neo1, 5′-CCACCAAAGAACGGAGCCGGTT-3′; SUMO-1,P3, 5′-CACTATGGATAAGACCTGTGAATT-3′). F_1 progeny was screened by PCR with primer pairs Neo1 and SUMO-1,P2. F_2 and subsequent generations were genotyped with primer pairs specific for targeted and wild-type *Sumo-1* alleles. Animals were of a mixed 129/SvEv and ICR background.

All mice were handled in accordance with the institutional animal care policy of the University of Helsinki. All animal protocols were approved by the University of Helsinki Review Board for Animal Experiments.

RNA isolation and preparation of cRNA probes. Total RNA was isolated from tissues or MEFs by using a NucleoSpin RNA II kit (Macherey-Nagel, Germany) or TRIzol reagent (Invitrogen, Carlsbad, CA) according to the manufacturers' instructions. ^{32}P-labeled or ^{35}S-labeled cRNA probes were synthesized by using the Riboprobe system II kit (Promega) for RNA blotting and in situ hybridization. DNA fragments generated by reverse transcription-PCR (RT-PCR), corresponding to nucleotides (nt) 104 to 359 of *Sumo-1* cDNA, nt 105 to 418 of *Sumo-3* cDNA (85% identical with nt 171 to 390 of *Sumo-2* cDNA), nt 412 to 662 of *Aos1* cDNA, nt 1490 to 1770 of *Uba2* cDNA, and nt 257 to 547 of *Ubc9* cDNA, were subcloned into the pGEM-T Easy vector (Promega) and used as templates. Ribosomal 28S rRNA cDNA probe was labeled with [^{32}P]CTP by random priming (Ready-To-Go DNA labeling beads; Amersham Biosciences).

RNA blotting. Portions (10 μg) of total RNA from different tissues or MEFs were resolved on 1.2% formaldehyde agarose gels and transferred onto nylon membranes (Hybond-XL; Amersham Pharmacia Biotech). The blot was hybridized with a ^{32}P-labeled antisense RNA probe (1.7×10^6 cpm/ml) for 2 h at 68°C in ULTRAhyb buffer (Ambion, Austin, TX). After high-stringency washes with 2× SSC (1× SSC is 0.15 M NaCl, 0.015 M sodium citrate) and 0.1% sodium dodecyl sulfate (SDS) (twice for 5 min at 68°C) and with 0.1× SSC and 0.1% SDS (twice for 15 min at 68°C), the membrane was exposed to Fuji X-ray film at −70°C for 24 to 72 h.

qRT-PCR. mRNAs encoding members of the SUMO protein family or proteins involved in the sumoylation pathway were quantified quantitative RT-PCR (qRT-PCR) (for the primers, see Table S1 in the supplemental material). cDNA was synthesized by using random hexamer primers with a Super-Script III first-strand synthesis kit (Invitrogen). Appropriate controls were included. qPCR was performed by using a LightCycler (Roche Diagnostics, Ltd., United Kingdom) in a 20-μl volume with 3.4 mM $MgCl_2$, 1 μM forward and reverse primers, and the LightCycler-DNA Master Sybr green I mix (Roche) according to the manufacturer's instructions. The PCR included an initial 10-s denaturation (95°C), followed by 41 to 45 cycles of 10-s denaturation (95°C), 5-s annealing (60 to 65°C), 10-s extension (72°C), and 5-s Sybr green I signal measurement (80 to 82°C). A DNA melting step was included after completion of PCR cycles to control for amplification specificity. The data were quantified by using LightCycler analysis software according to the manufacturer's instructions.

In situ hybridization. Sections (5 μm) of testis tissues at the different developmental stages were used for in situ hybridization. Sections were deparaffinized in xylene and rehydrated in descending concentrations of ethanol. Hybridization with antisense or sense probes was carried out in prehybridization solution containing 10% dextran sulfate and 0.5×10^5 to 1×10^5 cpm of cRNA probe/ml at 50°C for 4 h. After hybridization, tissue sections were treated for 30 min at 37°C with 10 μg of RNase A/ml, washed twice for 15 min at 50°C with 1× SSC, and dehydrated in a graded series of ethanol containing 0.3 M ammonium acetate (pH 5.2). The slides were coated with Kodak NTB-3 emulsion (Eastman Kodak Company, Rochester, NY) and stored at 4°C in light-tight boxes for 1 to 3 weeks. After development, the slides were counterstained with hematoxylin.

Histological analyses. *Sumo-1*$^{+/-}$ mice were mated, and the morning when the vaginal plug was found was defined as embryonic day 0 (E0). Embryos were dissected in phosphate-buffered saline, and palatal development was examined in situ under the dissection microscopy and recorded from E15 and E18. Embryos and testes, ovaries, and other organs were fixed in 4% paraformaldehyde at 4°C overnight, dehydrated, and embedded in paraffin. Paraffin blocks were sectioned at 5-μm thickness and stained with hematoxylin and eosin (BDH, Ltd., Poole, United Kingdom).

Immunoprecipitation and immunoblotting. For direct immunoblotting, tissue specimens and MEFs were homogenized in SDS-containing buffer (250 mM Tris-HCl [pH 6.8], 4% SDS, 10% glycerol, 2% β-mercaptoethanol, 1 mM dithiothreitol, and 1% protein inhibitor cocktail [Roche]), and the lysates were passed through 22- and 25-gauge needles several times. After the samples were heated at 100°C for 5 min, they were centrifuged at 13,000 rpm for 30 min at 4°C. Protein concentrations were determined by a modified Bradford assay (Bio-Rad Laboratories). Protein samples (10 to 12 μg) were electrophoresed on 4 to 20% polyacrylamide gradient gels (Lonza Rockland, Inc., ME) under denaturing conditions and transferred to nitrocellulose membranes. The primary antibodies used for immunoblotting were mouse anti-SUMO-1 monoclonal antibody (MAb) (Santa Cruz Biotechnology, Inc.), mouse anti-SUMO-1 MAb (Zymed Laboratories, San Francisco, CA), mouse anti-SUMO-2 MAb (Abnova, Tapei, Taiwan), mouse anti-VP-16 MAb (Santa Cruz Biotechnology, Inc.), and mouse anti-β-tubulin MAb (Santa Cruz Biotechnology, Inc.).

For immunoprecipitation experiments, MEFs and tissues were homogenized in radioimmunoprecipitation assay buffer (50 mM Tris-HCl [pH 7.8], 150 mM NaCl, 5 mM EDTA, 0.5% Triton X-100, 0.5% Nonidet P-40, 0.1% sodium deoxycholate, 1% protein inhibitor cocktail [Sigma], and 20 mM *N*-ethylmaleimide). Homogenates were clarified by centrifugation at 4°C for 10 min at 5,000 rpm and precleared by incubation with 50 μl of GammaBind Sepharose (Amersham Biosciences) for 30 min at 4°C on a rotary shaker. After centrifugation, the precleared supernatants were incubated with anti-SUMO-1 monoclonal MAb (Santa Cruz Biotechnology, Inc.), or anti-SUMO-2 MAb (Abnova) overnight at 4°C. After the addition of 50 μl of GammaBind Sepharose, the samples were incubated at 4°C for 1 h. The resin was washed four times with radioimmunoprecipitation assay buffer, and the pellets were resuspended in 2× SDS sample buffer. Immunoprecipitated proteins were resolved by SDS–12% polyacrylamide gel electrophoresis (PAGE), and immunoblotting was carried out by

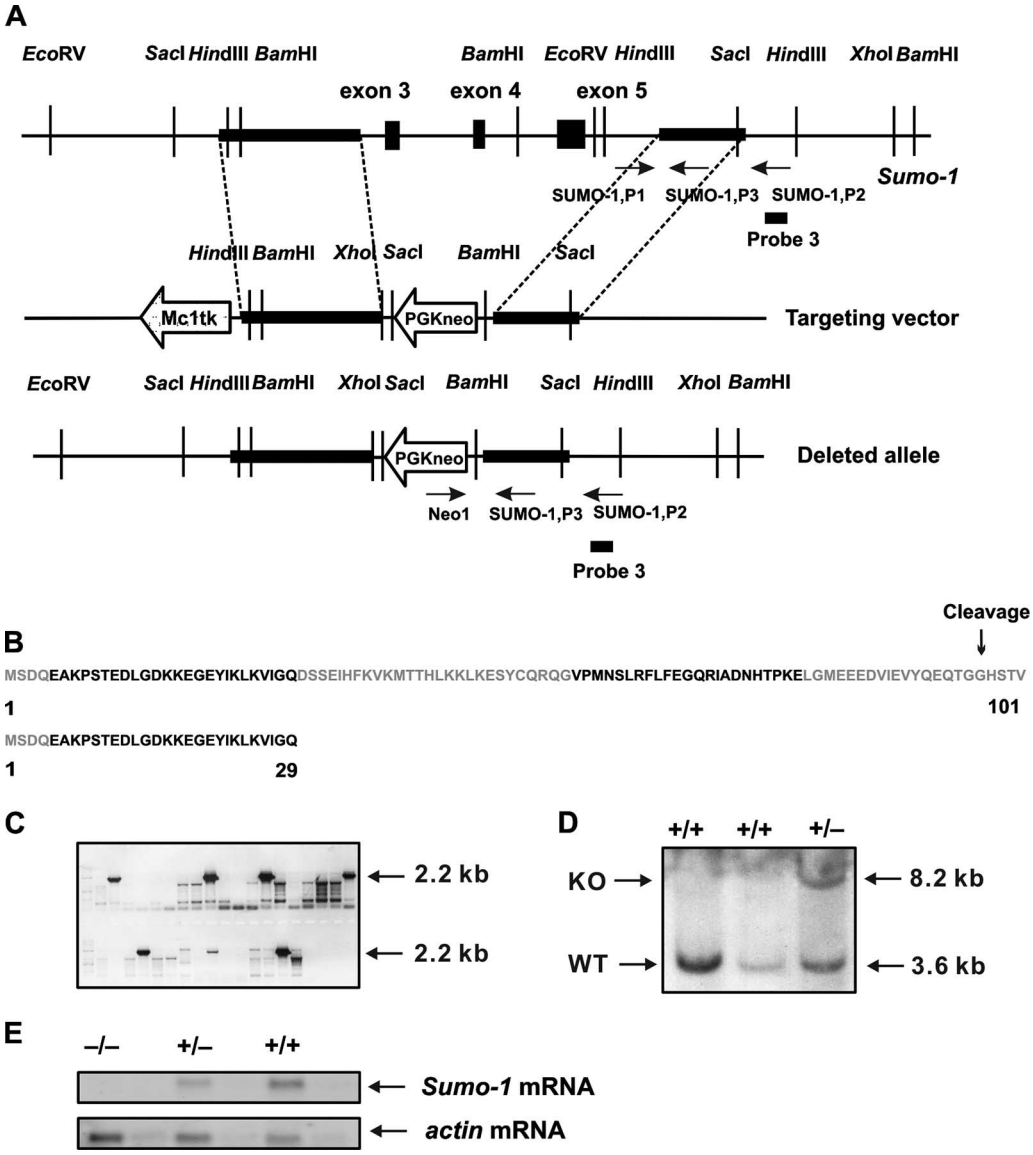

FIG. 1. Targeted disruption of the *Sumo-1* gene. (A) Replacement targeting vector to delete exons 3 to 5 of *Sumo-1*. The approximate locations of PCR primers used to screen for homologous recombinants and genotypes are shown (arrows) with the original and predicated structures of the gene after homologous recombination. The location of probe 3 used in Southern blotting is also depicted. (B) Amino acid sequence of SUMO-1. Color coding refers to the regions encoded by different exons of *Sumo-1*. The sequence of the 29-amino-acid long peptide that is potentially encoded by the targeted *Sumo-1* gene is shown below. (C) Positive ES clones were found to contain homologous recombination of *Sumo-1* by PCR screening using the primers Neo1 and SUMO-1,P2 shown in panel A. (D) Genomic DNA was isolated from two wild-type ES clones (WT) and one representative ES clone with homologous recombination of *Sumo-1* (KO), digested with HindIII, and analyzed by Southern blotting. The presence of both 3.2- and 8.6-kb bands indicates the presence of homologous recombination. (E) RNA blot hybridization analysis of samples isolated from testes of wild-type (+/+), heterozygous (+/−), and *Sumo-1*-deficient (−/−) mice with probes specific to *Sumo-1* and α-*actin* mRNA. The *Sumo-1* cRNA probe corresponds to nt 104 to 359 of *Sumo-1* mRNA and thus extends from 3′ end of exon 1 until 5′ end of exon 5 of the *Sumo-1* gene.

using polyclonal anti-RanGAP1 antibody (a gift from Frauke Melchior, Max-Planck Institute for Biochemistry, Munich, Germany).

Immunohistochemistry. Testes from 10- and 200-day-old mice were fixed overnight in 4% paraformaldehyde at 4°C, dehydrated, and embedded in paraffin using an automated tissue processor. Sections (5 μm thick) were mounted onto SuperFrost Plus slides (Menzel GmbH, Germany), dewaxed, and rehydrated. Endogenous peroxidase activity was blocked by incubation in 3% hydrogen peroxide in methanol. Slides were boiled for 15 min in 10 mM sodium citrate (pH 6.0) for antigen retrieval, washed in Tris-buffered saline (TBS), and blocked in TBS containing 1% bovine serum albumin (Sigma-Aldrich, St. Louis, MO) and 3% normal house or goat serum (Vector Laboratories, Burlingame, CA). Slides were incubated with primary antibody (anti-SUMO-1 [Santa Cruz Biotechnology]; anti-SUMO2+3 [ab3742; Abcam]) overnight at 4°C. After three washes in TBS, biotinylated anti-mouse immunoglobulin G diluted 1:100 was applied on sections and incubated for 1 h at room temperature. Visualization of the reaction was carried out by using the Vectastain Elite ABC and peroxidase DAB substrate kits (Vector Laboratories) according to the manufacturer's instructions. Slides were dehydrated in ascending ethanol series and mounted in Permount mounting medium (Fisher Chemicals, Fair Lawn, NJ).

MEF culture. MEFs were derived from 13.5-day-old wild-type and *Sumo-1*$^{-/-}$ embryos. After removal of the head and gastrointestinal tract, the embryos were washed with phosphate-buffered saline and minced, and the tissues were placed

into a 15-ml conical tube. A total of 50 ml of trypsin solution (0.025% trypsin, 1 mM EDTA) was added to the minced tissues, and cell suspensions were incubated at 37°C for 1 h with stirring. After centrifugation (1,000 rpm, 5 min), the cell pellets were washed twice with and resuspended in 10 ml of Dulbecco modified Eagle medium (DMEM) plus 10% fetal calf serum. Single-cell suspensions were plated onto 6-cm dishes that were incubated at 37°C for 2 to 3 days until confluence.

Adipocyte differentiation. MEFs were maintained in DMEM with 10% fetal bovine serum (FBS). For adipocyte differentiation, MEFs at passage 4 were cultured to confluence and treated with DMEM containing 10% FBS, 0.5 mM 3-isobutylmethylxanthine (Sigma), 10 μg of insulin (Sigma)/ml, 1 μM dexamethasone (Sigma), and 1 μM rosiglitazone (Cayman Chemical) (day 0). From day 2 on, the cells were treated with DMEM supplemented with 10% FBS, 10 μg of insulin/ml, and 1 μM rosiglitazone, refreshing the medium every 2 days. On day 10, the cells were fixed with 10% formaldehyde for 15 min at room temperature, and lipids were stained with Oil Red O and washed twice with water.

Cell proliferation assay. Cells (0.25×10^4 and 1×10^4 cells) were plated in triplicate onto 96-well flat-bottom dishes, Alamar Blue (20 μl) (BioSource, Germany) was added 20 h later, and the absorbance at 560 nm was recorded 2, 4, 8, 20, 24, 30, and 48 h thereafter.

RESULTS

Generation of *Sumo-1* knockout mice. The murine *Sumo-1* gene is located on chromosome 1, comprises 5 exons and 4 introns, and spans ~12 kb. Replacement of exons 3, 4, and 5 of *Sumo-1* with the neomycin resistance gene was used as the targeting strategy (Fig. 1A). The deleted exons 3, 4, and 5 correspond to amino acid residues 30 to 101 of the SUMO-1 protein. SUMO-1 is synthesized as an 101-residue precursor that undergoes maturation by proteolytic cleavage of the four most C-terminal residues (Fig. 1B), which exposes two C-terminal glycines (residues 96 and 97) that are essential for isopeptide bond formation to a lysine ε-amino group of target proteins (13, 16). Should the truncated *Sumo-1* mRNA be translated in vivo, the encoded polypeptide includes the first 29 N-terminal residues of the SUMO-1 protein and is devoid of a C-terminal glycine residue pair (Fig. 1B). The 29 N-terminal amino acid residues have not been assigned a role in SUMO-1 function; in other SUMO paralogues, there is a SUMO acceptor site in this region for potential formation of SUMO chains (13).

After electroporation of the targeting construct into ES cells and selection pressure, 125 surviving colonies were picked and screened by PCR. Five clones contained a 2.2-kb fragment in PCR analysis (Fig. 1C) and bands of expected size in Southern blots [3.6 kb for the wild-type and 8.2 kb for the targeted allele (Fig. 1D)], revealing that homologous recombination had occurred. *Sumo-1*$^{+/-}$ ES cells were morula aggregated with ICR morulae and implanted into pseudopregnant recipients. Germ line transmission was achieved by cross-breeding male chimeras with ICR females. Heterozygous mice were viable and fertile. Intercrosses of F_1 heterozygotes yielded F_2 progeny. Analyses of RNA isolated from testis, known to contain a high level of *Sumo-1* mRNA, revealed the presence of the 1.8-kb *Sumo-1* mRNA band in wild-type and heterozygous but not in *Sumo-1*$^{-/-}$ mice, indicating that deletion of *Sumo-1* had taken place. The amount of *Sumo-1* mRNA in heterozygous testis was reduced to about one-half of that in wild-type testis (Fig. 1E).

Phenotype of the animals. Intercrosses of heterozygous animals produced *Sumo-1*$^{+/+}$, *Sumo-1*$^{+/-}$, and *Sumo-1*$^{-/-}$ litters on a mixed 129SvEv-ICR genetic background. Of 542 pups born and examined at the age of 3 to 4 weeks, 153 were *Sumo-1*$^{+/+}$, 279 were *Sumo-1*$^{+/-}$, and 110 were *Sumo-1*$^{-/-}$. Genotype analysis of E15 and E18 embryos from heterozygous breeding indicated that of the 67 embryos examined, 18 were *Sumo-1*$^{+/+}$, 33 were *Sumo-1*$^{+/-}$, and 16 were *Sumo-1*$^{-/-}$. These numbers are compatible with Mendelian ratios expected for nondeleterious alleles. Thus, *Sumo-1* is not essential for embryonic development or viability of adult animals. *Sumo-1*$^{+/+}$ and *Sumo-1*$^{-/-}$ mice were identical upon gross examination. Development of body weights of *Sumo-1*$^{-/-}$ and wild-type littermates over a 12-month period were indistinguishable (Fig. 2). Histological analysis of various tissues failed to reveal any significant differences between *Sumo-1*$^{-/-}$ and wild-type mice or any obvious defects in tissues with normally high SUMO-1 expression, such as brain, lung, spleen, and testis tissues (data not shown). Likewise, there was no difference in cell proliferation rates between wild-type and *Sumo-1*$^{-/-}$ MEFs (data not shown). *Sumo-1*-targeted mice of both sexes, together with their wild-type littermates, were analyzed at the German Mouse Clinic (GSF National Research Center for Environment and Health, Neuherberg, Germany) in extensive screens for differences in gross anatomy, pathology, bone and cartilage morphology, nervous system morphology, clinical chemical analysis of blood and urine, energy metabolism, immunology and allergy, nociception, molecular phenotyping, and behavior. No differences were found between wild-type and *Sumo-1*$^{-/-}$ mice in these comprehensive screens except for nociception, in which a subtle difference was detected.

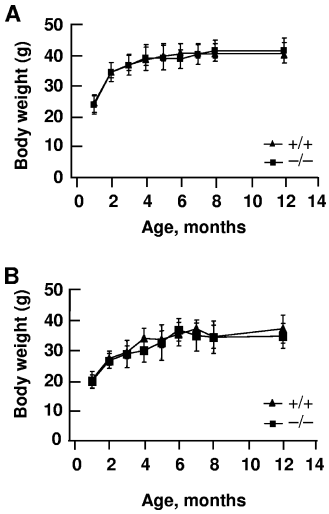

FIG. 2. Postnatal growth rate of mice wild-type an *Sumo-1*-null mice. The body weights of male (A) and female (B) littermates were recorded over a 12-month period. There were at least six male and female mice of each genotype. Wild-type, +/+; *Sumo-1*$^{-/-}$, −/−. Mean ± standard error of the mean (SEM) values are shown.

Expression of *Sumo-1 and Sumo-2/3* mRNA in MEFs and tissues. To validate further that *Sumo-1* targeting indeed yielded *Sumo-1*-null mice, *Sumo-1* mRNA expression was examined in *Sumo-1*$^{+/+}$ and *Sumo-1*$^{-/-}$ MEFs. *Sumo-1* mRNA was clearly detectable in *Sumo-1*$^{+/+}$ but not in *Sumo-1*$^{-/-}$ MEFs, whereas there was no difference in *Sumo-2/3* mRNA expression levels between *Sumo-1*$^{+/+}$ and *Sumo-1*$^{-/-}$ MEFs (see Fig. S1 in the supplemental material). *Sumo-1* mRNA was

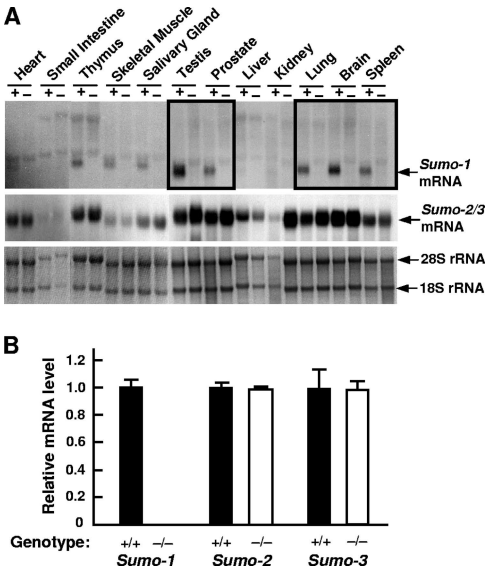

FIG. 3. *Sumo-1* and *Sumo-2/3* mRNA levels in wild-type and *Sumo-1*$^{-/-}$ mice. (A) RNA blot analysis of *Sumo-1* mRNA and *Sumo-2/3* mRNA levels in the different tissues from adult wild-type (+) and *Sumo-1*$^{-/-}$ (–) mice. The bottom panel depicts 28S and 18S rRNAs in the corresponding samples. (B) Quantitative RT-PCR analysis of *Sumo-1*, *Sumo-2*, and *Sumo-3* mRNA abundance in the testes of adult mice. The values were normalized by *Wbscr1* mRNA levels, and the results are expressed as mean ± SEM values of three individual samples. The mean wild-type value was 1.0.

expressed in all tissues examined in wild-type animals but not in *Sumo-1*$^{-/-}$ animals; in wild-type mice, its abundance was highest in the testis, brain, lungs, and spleen (Fig. 3A). *Sumo-2/3* mRNA was also present in all tissues examined, and there was no clear difference between wild-type and *Sumo-1*-targeted mice (Fig. 3A). Note that renal RNA from wild-type mice was somewhat degraded and loaded in smaller amounts than that from *Sumo-1*-null mice. That there was no compensatory increase in *Sumo-2* or *Sumo-3* mRNA abundance was further confirmed by qRT-PCR analyses of testis and renal RNA from wild-type and *Sumo-1*-targeted mice, and no increase was detected in *Sumo-2* or *Sumo-3* mRNA abundance in *Sumo-1*$^{-/-}$ testis (Fig. 3B) or kidney tissues (not shown).

Analysis of SUMO-1- and SUMO-2-modified proteins. Immunoblotting of lysates from MEFs with anti-SUMO-1 antibody revealed one major sumoylated band with a molecular mass of ~90-kDa in wild-type but not in *Sumo-1*$^{-/-}$ lysates. The same band was detected in testis of wild-type but not in *Sumo-1*-null mice (indicated by an asterisk in Fig. 4A). In addition, a band with the M_r of free SUMO-1 was visible, especially after a longer exposure time in both testis and MEF lysates of wild-type but not of *Sumo-1*-null mice (depicted by arrowheads in Fig. 4A). Similar results were seen in lysates from other tissues, such as the kidneys, liver, and brain, and also using another anti-SUMO-1 MAb (data not shown). Several other quite intense bands were visible in testis lysates after immunoblotting with anti-SUMO-1 MAb; however, the same bands were also detectable by anti-VP16 MAb (Fig. 4C) and thus correspond to proteins unrelated to SUMO-1. Immunoblotting of MEF and testis lysates with anti-SUMO-2 MAb revealed not only the presence of a band corresponding to the M_r of free SUMO-2 (depicted by an arrow in Fig. 4B) but also a more intensively stained ~90-kDa band in *Sumo-1*-null mice than in wild-type mice (indicated by an asterisk in Fig. 4B).

RanGAP1 is the most abundant cellular protein modified by SUMO-1 conjugation (24). That the ~90-kDa band seen in testis and MEF lysate blots (Fig. 4A and B) indeed corresponds to the sumoylated form of RanGAP1 was verified by using anti-RanGAP1 antibody on the same blot (data not shown). To validate further that RanGAP1 is not conjugated to SUMO-1 in *Sumo-1*$^{-/-}$ mice, soluble MEF extracts from wild-type and *Sumo-1*$^{-/-}$ were immunoprecipitated with anti-SUMO-1 or anti-SUMO-2 MAb (Fig. 5). Immune complexes were resolved by SDS-PAGE and immunoblotted with anti-RanGAP1 antibody. The ~90-kDa sumoylated RanGAP1

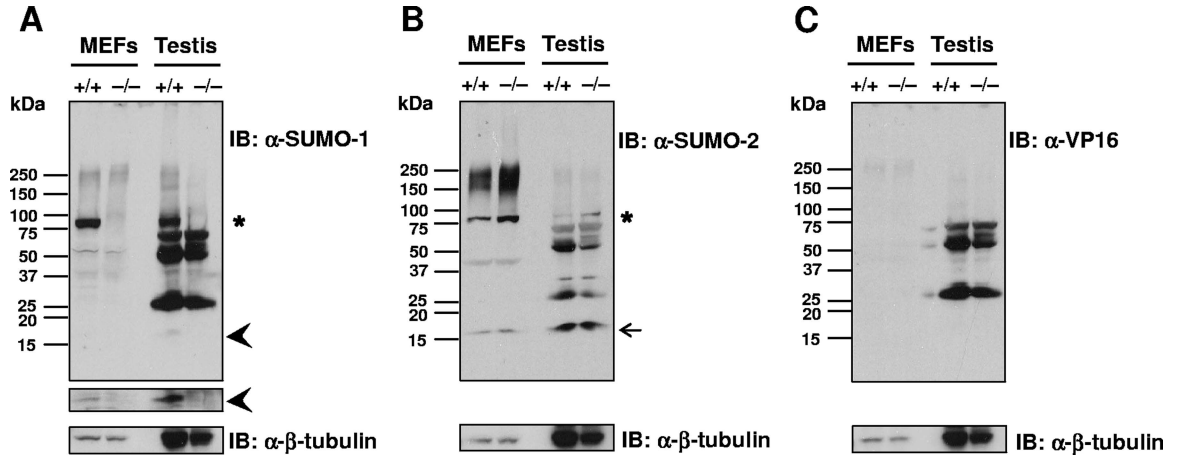

FIG. 4. Absence of SUMO-1-conjugated proteins and free SUMO-1 in MEF and testis lysates of wild-type and *Sumo-1*-null mice. Proteins in cell lysates were resolved by electrophoresis on 4 to 20% polyacrylamide gradient gels under denaturing conditions and transferred to nitrocellulose membranes. Panels A to C show immunoblots (IB) with anti-SUMO-1 antibody (A), anti-SUMO-2 antibody (B), and anti-VP16 antibody (C). In panel A, the narrow strip shows the free SUMO-1 region after a 10-fold longer exposure than for the main immunoblot. Anti-β-tubulin IB is shown for comparison in each instance. Asterisks depict the ~90-kDa band corresponding to sumoylated RanGAP1; arrowheads mark free SUMO-1, and the arrow identifies free SUMO-2.

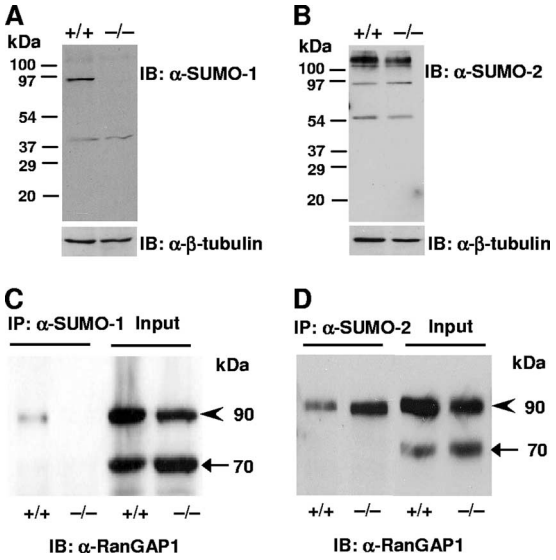

FIG. 5. Immunoblot analysis of SUMO-1, SUMO-2 and RanGAP1 proteins in wild-type and *Sumo-1*$^{-/-}$ MEFs. (A and B) Immunoblots of lysates from wild-type and *Sumo-1*$^{-/-}$ MEFs were generated by using anti-SUMO-1 antibody (A) or anti-SUMO-2 antibody (B). (C and D) MEFs lysates were immunoprecipitated with anti-SUMO-1 antibody (C) or anti-SUMO-2 antibody (D), after which the antibody-antigen complexes were resolved by electrophoresis on a 12% SDS gel and immunoblotted with anti-RanGAP1 antibody. IB, immunoblotting; IP, immunoprecipitation. The molecular mass of RanGAP1 is ~70 kDa (arrow) and that of sumoylated RanGAP1 is ~90 kDa (arrowhead).

band was detectable in wild-type but not in *Sumo-1*$^{-/-}$ MEFs after immunoprecipitation with anti-SUMO-1 antibody (Fig. 5C). However, RanGAP1 was conjugated to SUMO-2 in both wild-type and *Sumo-1*$^{-/-}$ MEFs, as judged by immunoprecipitation with anti-SUMO-2 antibody (Fig. 5D). It is of note that RanGAP1 is conjugated to a greater extent with SUMO-2 in *Sumo-1*-null MEFs than in wild-type MEFs. Comparable results were seen in experiments with liver extracts from wild-type and *Sumo-1*$^{-/-}$ *mice*. Thus, even though RanGAP1 is preferentially conjugated to SUMO-1 in cells, SUMO-2 is also its bona fide conjugation partner in vivo. A similar conclusion was also reached in quantitative proteomics analyses of HeLa cells expressing His_6-tagged SUMO-1 and SUMO-2 (43).

Palate development in *Sumo-1*$^{-/-}$ mice. *Sumo-1* haploinsufficiency was recently reported to result in the development of cleft lip and palate in humans and mice (3). Our results fail to confirm this report. We monitored palate development in *Sumo-1* mutant mice throughout embryonic development and found that the secondary palate was not totally closed at E15, but there was no clear morphological difference among *Sumo-1*$^{+/+}$, *Sumo-1*$^{+/-}$, and *Sumo-1*$^{-/-}$ embryos (data not shown). At E18.5, the secondary palate was properly fused in 43 of 44 embryos examined (wild-type, $n = 10$; heterozygotes, $n = 22$; and null, $n = 11$) (Fig. 6A and B); interestingly, one wild-type embryo had a cleft palate. Serial coronal sections of homozygous and heterozygous *Sumo-1* embryos at E18.5 confirmed that the closure of the palate was complete (Fig. 6C and D). The sections also revealed normal development of the mandible, the incisor teeth, and the Meckel's cartilage (data not shown).

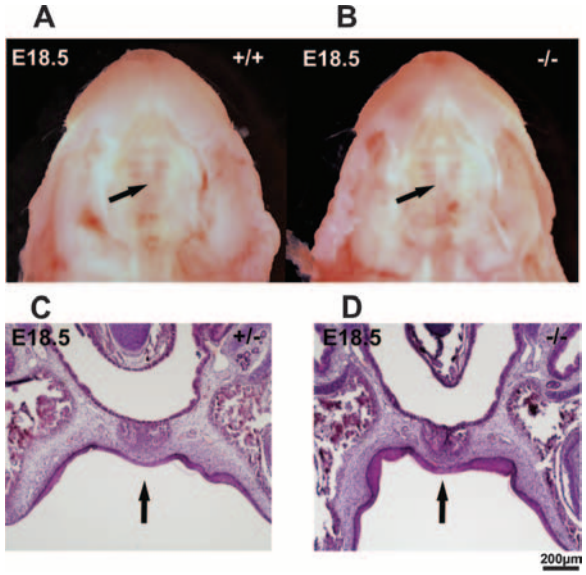

FIG. 6. Ventral view of the palatal region of wild-type and homozygous embryos at E18.5. Secondary palate (indicated by arrows) was closed in wild-type (A) and *Sumo-1*$^{-/-}$ (B) embryos. Histological sections confirm complete palate closure in a *Sumo-1* heterozygote (C) and homozygote embryo (D). Arrows indicate the midline of the palate where the two palatal shelves have fused.

Normal adipogenesis in the absence of SUMO-1. Conjugation of PPARγ specifically to SUMO-1 and liver X receptor specifically to SUMO-2/3 has been shown to enable independent control of transrepression pathway during repression of inflammation (14, 29, 32). In view of the fact that PPARγ is the master regulator of adipogenesis, it was pertinent to examine the consequence of SUMO-1 depletion in adipocyte differentiation. To this end, wild-type and *Sumo-1*$^{-/-}$ MEFs were obtained from embryos from the same litter and were induced to differentiate into adipocytes in vitro by using a medium containing isobutylmethylxanthine, dexamethasone, and insulin, followed by addition of insulin every 2 days (6). Adipocyte differentiation, as judged by lipid accumulation, was indistinguishable between wild-type and *Sumo-1*$^{-/-}$ MEFs (Fig. 7A). Upregulation of *PPARγ* and *aP2* expression represents a specific marker for adipogenesis, and qRT-PCT analysis revealed that accumulation of *PPARγ* and *aP2* mRNAs during adipogenesis was identical in wild-type and *Sumo-1*$^{-/-}$ MEFs (Fig. 7B). Thus, adipogenic differentiation and, by inference PPARγ function, is not dependent on conjugation to SUMO-1.

Reproductive function of *Sumo-1*-targeted mice. The reproductive system is an important SUMO target during postembryonic development in *C. elegans* (8), and *Sumo-1* mRNA is highly expressed in mouse testis. It was, therefore, important to examine whether the *Sumo-1*-null phenotype compromised male or female fertility. Breeding of *Sumo-1*$^{-/-}$ male or female mice with wild-type females or males produced litter sizes identical with those of wild-type mouse breeding at 8 weeks and 6 months of age, indicating that the loss of *Sumo-1* does not attenuate male and female fertility. *Sumo-1*$^{-/-}$ testis revealed the presence of normal spermatogenesis and spermatids in tubules. There was no apparent difference in Leydig cell morphology between wild-type and *Sumo-1*$^{-/-}$ testes. Like-

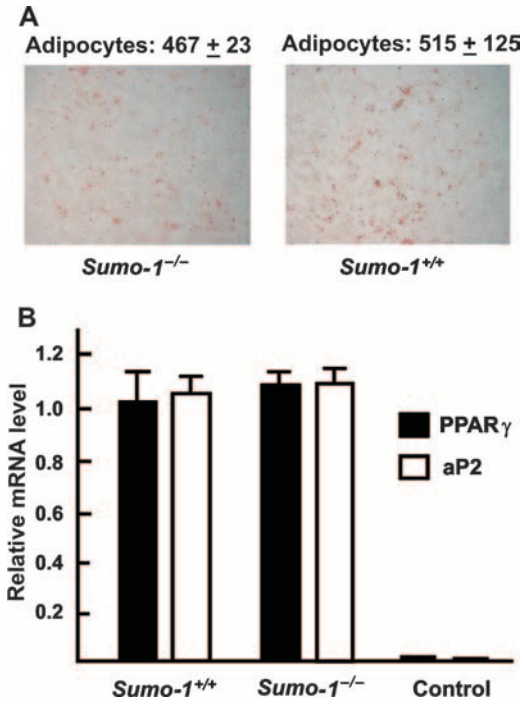

FIG. 7. Adipocyte differentiation of wild-type and *Sumo-1*$^{-/-}$ MEFs. Two days after reaching the confluence, the MEFs were induced to differentiate into adipocytes. (A) Cells were stained with Oil Red at 10 days after induction. Adipocyte numbers were counted from eight randomly selected fields from four dishes and were 515 ± 125 (SEM) and 467 ± 23 (SEM) for wild-type and *Sumo*-null MEFs, respectively. (B) Levels of *PPARγ* and *aP2* mRNAs in adipocytes differentiated for 10 days from wild-type and *Sumo-1*$^{-/-}$ MEFs. "Control" refers to MEFs that were cultured in the absence of differentiation medium. The values were normalized by *Gapdh* mRNA levels, and the results are expressed as mean ± SEM values of three samples.

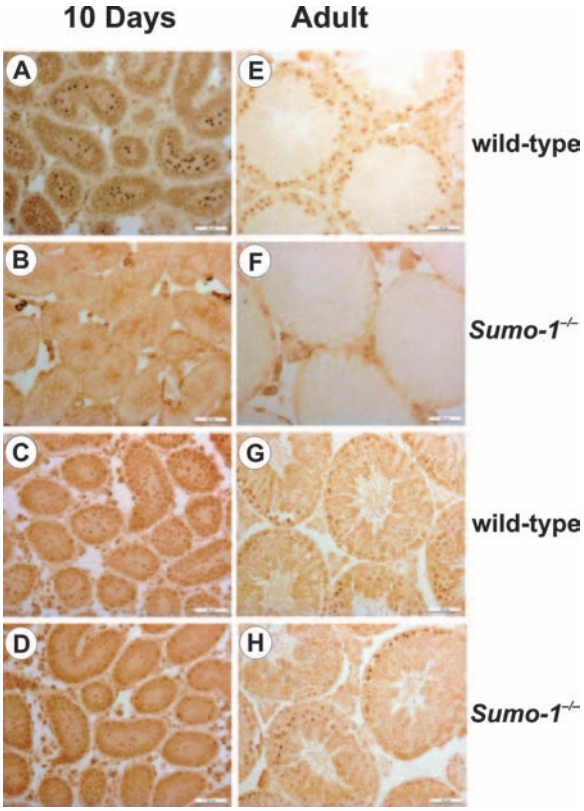

FIG. 8. Immunohistochemical analyses of SUMO-1 (A, B, E, and F) and SUMO-2/3 (C, D, G, and H) antigens in the testes of wild-type (A, C, E, and G) and *Sumo-1*$^{-/-}$ (B, D, F, and H) mice at 10 days of age (10 days) and in adulthood (adult). XY bodies are depicted by the dark brown spots within the semineferous tubules. Bar, 50 μm.

wise, the ovaries of *Sumo-1*$^{-/-}$ female at 8 weeks of age showed normal follicular development and corpora lutea (see Fig. S2 in the supplemental material).

Expression of sumoylation pathway genes during testis development. SUMO-1 has been shown to be located on the sex chromosomes of meiotic spermatocytes, the centrosome, and manchette of spermatids (30, 44), but little is known about the role of sumoylation during testis development. The abundance of *Sumo-1 Aos1*, *Uba2*, and *Ubc9* mRNAs was low in newborns and increased with age, reaching the highest level at adulthood (see Fig. S3 and S4 and other results in the supplemental material). In contrast, *Sumo-2/3* expression was high already in newborns (see Fig. S3 in the supplemental material). *Sumo-1* mRNA was present in all germ cells, except for elongating spermatids, whereas the presence of *Sumo-2/3* mRNA was restricted to pachytene spermatocytes. SUMO-1 protein was detected in a subnuclear compartment of pachytene spermatocytes called the XY body in adult wild-type testis, but not in *Sumo-1*$^{-/-}$ testis (Fig. 7). SUMO-2/3 antigen was found in the developing (day 10) and adult XY body both in wild-type and in *Sumo-1*$^{-/-}$ testes, and the expression pattern of SUMO-2/3 was the same in wild-type and *Sumo-1-null* testes (Fig. 8).

Knockdown of the *Piasx* gene encoding the SUMO E3 ligase PIASxα/β results in a mild testicular phenotype (34). It was, therefore, of interest to examine whether any compensatory changes occurred in expression of sumoylation pathway genes during testis development of in *Sumo-1*$^{-/-}$ mice, because *Sumo-1*-targeted mice failed to present a testicular phenotype. However, the abundance of *Aos1*, *Uba2*, *Ubc9*, *Pias1*, *Pias3*, *Piasx*, and *Piasy* mRNAs was very similar in *Sumo-1*$^{+/+}$ and *Sumo-1*$^{-/-}$ testes (see Fig. S5 in the supplemental material). In view of these results, we conclude that SUMO-1 is dispensable in normal testis development, and its lack is compensated for by other SUMO paralogues without upregulation of other components in the sumoylation pathway.

DISCUSSION

Sumoylation is a biologically important and reversible protein modification, with its target proteins being associated with multiple cellular functions. Four members belong to the SUMO protein family in mammals, SUMO-1 to SUMO-4, and each member is encoded by a distinct *Sumo* gene (16, 23). In cells, the majority of SUMO-1 is conjugated to substrates, but there is a significant pool of free SUMO-2/3 that is rapidly converted to conjugated high-M_r species in response to a variety of cellular stresses (33). Even though most of the SUMO substrates do not differentiate between SUMO-1 and SUMO-2 as the conjugation partner in cell-free experiments with recombinant enzymes or under ectopic expression conditions, it is

nevertheless assumed that SUMO family proteins are preferentially conjugated to different substrates under physiological conditions. For example, RanGAP1 is preferentially modified by SUMO-1 (33, 39) and topoisomerase II by SUMO-2/3 (4, 5), whereas the promyelocytic leukemia protein is conjugated to both SUMO-1 (25) and SUMO-2/3 (12). In HeLa cells stably expressing His_6-SUMO-1 or His_6-SUMO-2, quantitative proteomics analysis revealed that 25 proteins were preferentially conjugated to SUMO-1, 19 proteins were preferentially conjugated to SUMO-2, and 9 proteins were preferentially conjugated to both SUMO-1 and SUMO-2 (43). Although many targets have been shown to exhibit SUMO paralogue preference in these studies and other similar experiments (13, 15, 19, 47), the extent to which the SUMO family members are redundant in their in vivo functions is not clear. As the first step toward understanding this issue along with the overall biological importance of SUMO-1, we generated *Sumo-1*-null mice and show here that the functions of SUMO-1 are dispensable in normal mouse development. Other SUMO paralogues are likely able to compensate for the loss of SUMO-1 in vivo, as exemplified in the present study by showing increased RanGAP1 conjugation to SUMO-2 in *Sumo-1*-null mice in comparison to wild-type mice. Importantly, compensation for *Sumo-1* loss occurred without any apparent upregulation in the expression of other SUMO paralogues or members of the sumoylation pathway.

A recent study reported the presence of cleft palate or oblique facial cleft of low penetrance in *Sumo-1* heterozygote pups and embryos, and demise of both heterozygotes and homozygotes between E13.5 and E18.5, as well as during the immediate postnatal period (3). Our results disagree with this report in that genotype analysis of E15 and E18 embryos from *Sumo-1* heterozygote breeding showed the predicted Mendelian ratios for $Sumo\text{-}1^{+/+}$, $Sumo\text{-}1^{+/-}$, and $Sumo\text{-}1^{-/-}$ genotypes. The same applied to genotypes of *Sumo-1*-targeted mice at the age of 3 to 4 weeks. Formation of the mammalian secondary palate is a dynamic process (48). Palatal shelves are observed in E13.5 embryos as they grow out from the maxillary processes on either side of the tongue. At E14.5, the palatal shelves on both sides are elevated to a horizontal position dorsal to the tongue and abutted each other. By E16.5, the medial-edge epithelia approximating the palatal shelves from the two sides complete fusion and are then degenerated, resulting in an intact palate. The phenotype of cleft palate can result from an impairment at any of the above steps. We found these events to proceed normally in embryos with all genotypes and failed to observe any connection between *Sumo-1* genotype and palatal development. The report of Alkuraya et al. (3) provides scanty details of the ways by which the *Sumo-1* gene was interrupted by a gene trap construct and, therefore, it cannot be judged whether functions of other genes were also influenced by their targeting strategy. Since mice of different genetic backgrounds were used in our study and that of Alkuraya et al. (3), we cannot formally rule out the possibility that genetic background modifies the outcome of *Sumo-1* disruption. Nevertheless, our results show unequivocally that *Sumo-1* function is dispensable in normal mouse embryonic development, including palate formation.

Similar to ubiquitination, sumoylation is a multistep process and is mediated by distinct E1, E2, and E3 activities (16, 19). Sumoylation relies on a single E2 conjugating enzyme, Ubc9, encoded by a highly conserved gene. In *S. cerevisiae*, Ubc9-depleted cells arrest in G_2/M phase, causing the accumulation of large budded cells with a single nucleus, a short spindle, and replicated DNA (35). In contrast, hus5 (Ubc9 homolog) deletion is viable in *Schizosaccharomyces pombe*, but cells are severely impaired in growth and exhibit high levels of abortive mitosis and chromosome mis-segregation (2), a phenotype closely resembling that of pmt3 (SUMO homolog) loss (41). *Ubc9*-null mouse embryos die at the early postimplantation stage. Mutant cells show chromosome defects and gross alterations in nuclear organization, misshapen nuclei, as well as mislocalized RanGAP1 and Ran (26). These results indicate that Ubc9 and, by implication, sumoylation are essential for mouse embryonic viability and formation of proper nuclear architecture. Moreover, fine-tuned balance of SUMO modifications seems essential for mammalian development, as revealed by mutation of the mouse *Senp1* gene (46). Our present findings do not question the importance of sumoylation in mouse development; rather, our results indicate that different SUMO paralogues encoded by distinct genes have redundant functions in vivo.

There are four *Pias* family members in mammals—*Pias1*, *Pias3*, *Piasx*, and *Piasy*—that encode potential E3 ligases in the sumoylation pathway (38). However, these proteins most likely have also other distinct functions unrelated to their E3 ligase activity (28, 37). For example, studies of $Pias1^{-/-}$ mice demonstrated that PIAS1 function is important in innate immunity (22). $Piasy^{-/-}$ mice appeared phenotypically normal (45), although signaling in responses to IFN-γ and Wnt agonists was modestly attenuated in $Piasy^{-/-}$ cells. We have previously reported that there is a mild testicular phenotype in $Piasx^{-/-}$ mice that are phenotypically otherwise normal (34). We crossed $Sumo\text{-}1^{-/-}$ and $Piasx^{-/-}$ mice to generate double-knockout $Sumo\text{-}1^{-/-}$ $Piasx^{-/-}$ animals to evaluate whether the absence of SUMO-1 exacerbated the $Piasx^{-/-}$ phenotype. This was not observed; rather, the testicular phenotype of $Sumo\text{-}1^{-/-}$ $Piasx^{-/-}$ mice was essentially the same as that of *Piasx*-null mice (L. Mikkonen, F.-P. Zhang, and O. A. Jänne, unpublished results). In addition, the expression of the genes encoding PIAS family members was not upregulated in testis of *Sumo-1*-null mice, suggesting that these proteins are not rate-limiting in the sumoylation pathway.

PPARγ is both necessary and sufficient for adipogenesis and normal glucose homeostasis and also exerts broad anti-inflammatory effects in macrophages and other cell types (14, 29, 31). Ectopic expression of PPARγ is sufficient to induce adipocyte differentiation in fibroblasts, and no factor has been found that promotes adipogenesis in the absence of PPARγ (42). *PPARγ*-null mice have decreased adipose tissue mass, and MEFs from these animals have impaired adipogenesis (49). Recent studies showed that the PPARγ-dependent transrepression pathway is initiated by ligand-induced SUMO-1 conjugation of the ligand-binding domain of PPARγ (29). Our results demonstrated that the ability of $Sumo\text{-}1^{-/-}$ MEFs to differentiate into adipocyte was not significantly different from that of wild-type MEFs. Likewise, there was no significant difference in body weight development between $Sumo\text{-}1^{-/-}$ and wild-type mice. It is thus likely that sumoylation of PPARγ by SUMO-1 is not essential

for its function or that PPARγ can be sumoylated by other SUMO paralogues during adipocyte differentiation.

In summary, our characterization of *Sumo-1*-null phenotype in mice indicates that SUMO-1 is not essential for mouse development and that potential in vivo functions of SUMO-1, including those exerted either by covalent conjugation or through noncovalent interactions, are compensated for by other SUMO paralogues. This knowledge is of great importance for attempts aimed at targeting the sumoylation pathway for therapeutic purposes.

ACKNOWLEDGMENTS

We thank Saija Kotola, Johanna Iso-Oja, and Katja Kiviniemi for excellent technical assistance; the personnel of the animal facility for taking care of the mice; and Katja Helenius for advice in adipocyte differentiation experiments. We are grateful to the German Mouse Clinic (GSF National Research Center for Environment and Health, Neuherberg, Germany) for phenotype screening of *Sumo-1*-targeted mice.

This study was supported by grants from the Academy of Finland, Biocentrum Helsinki, the Sigrid Jusélius Foundation, the Finnish Foundation for Cancer Research, the Paulo Foundation, the Oskar Öflund Foundation, the Finnish Medical Foundation, Helsinki University Central Hospital, the Research and Science Foundation of Farmos, and the European Union (contract no. LSHM-CT-2005-018652).

REFERENCES

1. **Alarcon-Vargas, D., and Z. Ronai.** 2002. SUMO in cancer—wrestlers wanted. Cancer Biol. Ther. **1:**237–242.
2. **Al-Khodairy, F., T. Enoch, I. M. Hagan, and A. M. Carr.** 1995. The *Schizosaccharomyces pombe hus5* gene encodes a ubiquitin conjugating enzyme required for normal mitosis. J. Cell Sci. **108:**475–486.
3. **Alkuraya, F. S., I. Saadi, J. J. Lund, A. Turbe-Doan, C. C. Morton, and R. L. Maas.** 2006. SUMO1 haploinsufficiency leads to cleft lip and palate. Science **313:**1751.
4. **Azuma, Y., A. Arnaoutov, T. Anan, and M. Dasso.** 2005. PIASy mediates SUMO-2 conjugation of topoisomerase-II on mitotic chromosomes. EMBO J. **24:**2172–2182.
5. **Azuma, Y., A. Arnaoutov, and M. Dasso.** 2003. SUMO-2/3 regulates topoisomerase II in mitosis. J. Cell Biol. **163:**477–487.
6. **Baudry, A., Z. Z. Yang, and B. A. Hemmings.** 2006. PKBα is required for adipose differentiation of mouse embryonic fibroblasts. J. Cell Sci. **119:**889–897.
7. **Bebington, C., F. J. Doherty, and S. D. Fleming.** 2001. The possible biological and reproductive functions of ubiquitin. Hum. Reprod. Update **7:**102–111.
8. **Broday, L., I. Kolotuev, C. Didier, A. Bhoumik, B. P. Gupta, P. W. Sternberg, B. Podbilewicz, and Z. Ronai.** 2004. The small ubiquitin-like modifier (SUMO) is required for gonadal and uterine-vulval morphogenesis in *Caenorhabditis elegans*. Genes Dev. **18:**2380–2391.
9. **Cheng, J., T. Bawa, P. Lee, L. Gong, and E. T. Yeh.** 2006. Role of desumoylation in the development of prostate cancer. Neoplasia **8:**667–676.
10. **Dohmen, R. J.** 2004. SUMO protein modification. Biochim. Biophys. Acta **1695:**113–131.
11. **Domanskyi, A., K. T. Virtanen, J. J. Palvimo, and O. A. Jänne.** 2006. Biochemical characterization of androgen receptor-interacting protein 4. Biochem. J. **393:**789–795.
12. **Fu, C., K. Ahmed, H. Ding, X. Ding, J. Lan, Z. Yang, Y. Miao, Y. Zhu, Y. Shi, J. Zhu, H. Huang, and X. Yao.** 2005. Stabilization of PML nuclear localization by conjugation and oligomerization of SUMO-3. Oncogene **24:**5401–5413.
13. **Geiss-Friedlander, R., and F. Melchior.** 2007. Concepts in sumoylation: a decade on. Nat. Rev. Mol. Cell. Biol. **8:**947–956.
14. **Ghisletti, S., W. Huang, S. Ogawa, G. Pascual, M. E. Lin, T. M. Willson, M. G. Rosenfeld, and C. K. Glass.** 2007. Parallel SUMOylation-dependent pathways mediate gene- and signal-specific transrepression by LXRs and PPARγ. Mol. Cell **25:**57–70.
15. **Gill, G.** 2005. Something about SUMO inhibits transcription. Curr. Opin. Genet. Dev. **15:**536–541.
16. **Hay, R. T.** 2005. SUMO: a history of modification. Mol. Cell **18:**1–12.
17. **Hay, R. T.** 2007. SUMO-specific proteases: a twist in the tail. Trends Cell Biol. **17:**370–376.
18. **Jänne, O. A., A.-M. Moilanen, H. Poukka, N. Rouleau, U. Karvonen, N. Kotaja, M. Häkli, and J. J. Palvimo.** 2000. Androgen-receptor-interacting nuclear proteins. Biochem. Soc. Trans. **28:**401–405.
19. **Johnson, E. S.** 2004. Protein modification by SUMO. Annu. Rev. Biochem. **73:**355–382.
20. **Jones, D., E. Crowe, T. A. Stevens, and E. P. Candido.** 2002. Functional and phylogenetic analysis of the ubiquitylation system in *Caenorhabditis elegans*: ubiquitin-conjugating enzymes, ubiquitin-activating enzymes, and ubiquitin-like proteins. Genome Biol. **3:**RESEARCH0002.
21. **Li, M., D. Guo, C. M. Isales, D. L. Eizirik, M. Atkinson, J.-X. She, and C.-Y. Wang.** 2005. SUMO wrestling with type 1 diabetes. J. Mol. Med. **83:**504–513.
22. **Liu, B., S. Mink, K. A. Wong, N. Stein, C. Getman, P. W. Dempsey, H. Wu, and K. Shuai.** 2004. PIAS1 selectively inhibits interferon-inducible genes and is important in innate immunity. Nat. Immunol. **5:**891–898.
23. **Melchior, F.** 2000. SUMO—nonclassical ubiquitin. Annu. Rev. Cell Dev. Biol. **16:**591–626.
24. **Muller, S., C. Hoege, G. Pyrowolakis, and S. Jentsch.** 2001. SUMO, ubiquitin's mysterious cousin. Nat. Rev. Mol. Cell. Biol. **2:**202–210.
25. **Muller, S., M. J. Matunis, and A. Dejean.** 1998. Conjugation with the ubiquitin-related modifier SUMO-1 regulates the partitioning of PML within the nucleus. EMBO J. **17:**61–70.
26. **Nacerddine, K., F. Lehembre, M. Bhaumik, J. Artus, M. Cohen-Tannoudji, C. Babinet, P. P. Pandolfi, and A. Dejean.** 2005. The SUMO pathway is essential for nuclear integrity and chromosome segregation in mice. Dev. Cell **9:**769–779.
27. **Owerbach, D., E. M. McKay, Y. T. Yeh, K. H. Gabbay, and K. M. Bohren.** 2005. A proline-90 residue unique to SUMO-4 prevents maturation and sumoylation. Biochem. Biophys. Res. Commun. **337:**517–520.
28. **Palvimo, J. J.** 2007. PIAS proteins as regulators of small ubiquitin-related modifier (SUMO) modifications and transcription. Biochem. Soc. Trans. **35:**1405–1408.
29. **Pascual, G., A. L. Fong, S. Ogawa, A. Gamliel, A. C. Li, V. Perissi, D. W. Rose, T. M. Willson, M. G. Rosenfeld, and C. K. Glass.** 2005. A SUMOylation-dependent pathway mediates transrepression of inflammatory response genes by PPAR-γ. Nature **437:**759–763.
30. **Rogers, R. S., A. Inselman, M. A. Handel, and M. J. Matunis.** 2004. SUMO modified proteins localize to the XY body of pachytene spermatocytes. Chromosoma **113:**233–243.
31. **Rosen, E. D., and O. A. MacDougald.** 2006. Adipocyte differentiation from the inside out. Nat. Rev. Mol. Cell. Biol. **7:**885–896.
32. **Rosen, E. D., C. J. Walkey, P. Puigserver, and B. M. Spiegelman.** 2000. Transcriptional regulation of adipogenesis. Genes Dev. **14:**1293–1307.
33. **Saitoh, H., and J. Hinchey.** 2000. Functional heterogeneity of small ubiquitin-related protein modifiers SUMO-1 versus SUMO-2/3. J. Biol. Chem. **275:**6252–6258.
34. **Santti, H., A. Anand, S. Hirvonen-Santti, J. Toppari, M. Panhuysen, F. Vauti, M. Perera, G. Corte, W. Wurst, O. A. Jänne, and J. J. Palvimo.** 2005. Disruption of the murine PIASx gene results in reduced testis weight. J. Mol. Endocrinol. **34:**645–654.
35. **Seufert, W., B. Futcher, and S. Jentsch.** 1995. Role of a ubiquitin-conjugating enzyme in degradation of S- and M-phase cyclins. Nature **373:**78–81.
36. **Shao, R., F. P. Zhang, E. Rung, J. J. Palvimo, I. Huhtaniemi, and H. Billig.** 2004. Inhibition of small ubiquitin-related modifier-1 expression by luteinizing hormone receptor stimulation is linked to induction of progesterone receptor during ovulation in mouse granulosa cells. Endocrinology **145:**384–392.
37. **Sharrocks, A. D.** 2006. PIAS proteins and transcriptional regulation—more than just SUMO E3 ligases? Genes Dev. **20:**754–758.
38. **Shuai, K.** 2000. Modulation of STAT signaling by STAT-interacting proteins. Oncogene **19:**2638–2644.
39. **Sternsdorf, T., K. Jensen, and H. Will.** 1997. Evidence for covalent modification of the nuclear dot associated proteins PML and Sp100 by PIC1/SUMO-1. J. Cell Biol. **139:**1621–1634.
40. **Sutovsky, P., R. M. Turner, S. Hameed, and M. Sutovsky.** 2003. Differential ubiquitination of stallion sperm proteins: possible implications for infertility and re productive seasonality. Biol. Reprod. **68:**688–698.
41. **Tanaka, K., J. Nishide, K. Okazaki, H. Kato, O. Niwa, T. Nakagawa, H. Matsuda, M. Kawamukai, and Y. Murakami.** 1999. Characterization of a fission yeast SUMO-1 homologue, pmt3p, required for multiple nuclear events, including the control of telomere-length and chromosome segregation. Mol. Cell. Biol. **19:**8660–8672.
42. **Tontonoz, P., E. Hu, and B. M. Spiegelman.** 1994. Stimulation of adipogenesis in fibroblasts by PPARγ2, a lipid-activated transcription factor. Cell **79:**1147–1156.
43. **Vertegaal, A. C., J. S. Andersen, S. C. Ogg, R. T. Hay, M. Mann, and A. I. Lamond.** 2006. Distinct and overlapping sets of SUMO-1 and SUMO-2 target proteins revealed by quantitative proteomics. Mol. Cell Proteomics. **5:**2298–2310.
44. **Vigodner, M., and P. L. Morris.** 2005. Testicular expression of small ubiquitin-related modifier-1 (SUMO-1) supports multiple roles in spermatogenesis: silencing of sex chromosomes in spermatocytes, spermatid microtubule nucleation, and nuclear reshaping. Dev. Biol. **282:**480–492.
45. **Wong, K. A., R. Kim, H. Christofk, J. Gao, G. Lawson, and H. Wu.** 2004.

Protein inhibitor of activated STAT Y (PIASy) and a splice variant lacking exon 6 enhance sumoylation but are not essential for embryogenesis and adult life. Mol. Cell. Biol. **24:**5577–5586.
46. **Yamaguchi, T., P. Sharma, M. Athanasiou, A. Kumar, S. Yamada, and M. R. Kuehn.** 2005. Mutation of SENP1/SuPr-2 reveals an essential role for desumoylation in mouse development. Mol. Cell. Biol. **25:**5171–5182.
47. **Zhao, J.** 2007. Sumoylation regulates diverse biological processes. Cell Mol. Life Sci. **64:**3017–3033.
48. **Zhao, Y., Y.-J. Guo, A. C. Tomac, N. R. Taylor, A. Grinberg, E. J. Lee, S. P. Huang, and H. Westphal.** 1999. Isolated cleft palate in mice with a targeted mutation of the LIM homeobox gene lhx8. Proc. Natl. Acad. Sci. USA **96:**15002–15006.
49. **Zhang, J., M. Fu, T. Cui, C. Xiong, K. Xu, W. Zhong, Y. Xiao, D. Floyd, J. Liang, E. Li, Q. Song, and Y. E. Chen.** 2004. Selective disruption of PPARγ2 impairs the development of adipose tissue and insulin sensitivity. Proc. Natl. Acad. Sci. USA **101:**10703–10708.